

Kinship Verification through a Forest Neural Network

Ali Nazari, Mohsen Ebrahimi Moghaddam, Omidreza Borzoei

Faculty of Computer Science and Engineering, Shahid Beheshti University, Velenjak, Tehran, 1983969411, Tehran, Iran.

*Corresponding author(s). E-mail(s): m_moghadam@sbu.ac.ir;
Contributing authors: al_nazari@sbu.ac.ir; borzoei.omidreza@gmail.com;

Abstract

Early methods used face representations in kinship verification, which are less accurate than joint representations of parents' and children's facial images learned from scratch. We propose an approach featuring graph neural network concepts to utilize face representations and have comparable results to joint representation algorithms. Moreover, we designed the structure of the classification module and introduced a new combination of losses to engage the center loss gradually in training our network. Additionally, we conducted experiments on KinFaceW-I and II, demonstrating the effectiveness of our approach. We achieved the best result on KinFaceW-II, an average improvement of nearly 1.6 for all kinship types, and we were near the best on KinFaceW-I. The code is available at <https://github.com/ali-nazari/Kinship-Verification>

Keywords: Kinship Verification, Graph Neural Network, Forest Neural Network, Center loss

1 Introduction

Visual kinship verification receives two face images and indicates whether they have a family relationship. It has considerable potential to use in sociology, anthropology, psychology, neuroscience, genetics, privacy protection and social media [1–3] for example, finding missing family members [4], collecting photos for the family album [3], family privacy protection [5], border control and criminal investigation [1, 6]. Moreover, it has been recently investigated in smart environments to recognize family members [7].

Generally, there are two approaches to tackling the problem of kinship verification: face matching (joint representation) and face representation. In face matching or joint representation, two face images are processed jointly to determine their kinship relation [8]. Due to its effectiveness and performance in Kinship Verification (KV), the most recent research has utilized this approach and achieved the most advanced and competitive results in the field, often referred to as 'state-of-the-art results' [8, 9]. On the other hand, most early methods lay in the second approach and attempted first to analyze faces to obtain unique features as face representation. Then, their algorithms decided their kinship relation based on those face representations. This approach has some benefits as it uses the capabilities of a highly demanding application, i.e., face recognition (FR). For example, it does not need to retrain all data from scratch because we have each face's representation.

In addition, solutions based on face representation for KV are not accurate compared to the face matching methods [10]. We propose a method with high accuracy in KV based on the second approach and apply graph neural network concepts and the notion that corresponding facial components are related in paired images of family members, especially siblings [11–13].

To our knowledge, this paper is the first to apply graph neural network concepts to kinship verification. There are rare papers that use graph structures in kinship verification. Graph embedding-based metric learning [14] introduced an intrinsic graph and two penalty graphs to acquire multiple metrics. H-RGN [8] designed a tree-like structure by grouping feature elements as nodes and performing convolutional operations among them. Although these papers attempted to apply graph concepts, they did not completely use GNN concepts.

Our key contributions to elevate the accuracy of kinship verification are enumerated as follows:

- We propose the Forest Neural Network (FNN) considering the disjointing nature of face components and exchanging information among them through GNN operators.
- Our method can exploit various CNN networks, each as an expert system including an extension of CNN, Extended Residual Network (ERN), using the attention mechanism and producing a consistent representation with popular CNNs. It also benefits from high-resolution images to mitigate the differences in pixel values when facial images are taken under various conditions alongside providing detailed information
- A concerted combination of losses is introduced so that the center loss with other losses in this realm can condense the features of each class to classify easier and outperform previous studies.

The organization of this paper is as follows: Section 2 briefly expresses related work. The proposed algorithm is explained in Section 3. Section 4 provides experiments, their configuration, and the analysis sub-section to clarify various parts of the proposed algorithm. Eventually, Section 5 concludes the paper.

2 Related Work

Various approaches have been suggested to overcome kinship verification, from low-level and mid-level features to algorithms such as traditional machine learning, metric learning, deep learning, and hybrid models [1, 2].

Early methods are considered to employ detailed and complete facial information for the convenience of face analysis. Hence, early methods attempted to discover a description of faces, especially discriminatory features. Low-level features such as facial distances, gradient histograms, and color information were applied to determine the kinship relation [15].

Textural features, LBP variants [16], Gabor filter [17], salient facial features [18], self-similarity [19], and SIFT Flow [20] were also explored. Most papers using this approach used SVM as a classifier in the final stage. In a research [21], appearance and geometric features were applied. A pyramid of the face was constructed, and distances between similar blocks of paired images in pyramids were used as appearance features. In addition, geometric features and facial landmarks were employed to compute geodesic distances between two face images [21]. In the recent work [22], color and texture handcrafted techniques such as Heterogeneous Auto-similarities of Characteristics (HASC), Color Correlogram (CC), and Dense Color Histogram (DCH) were combined to increase the accuracy.

Regarding mid-level features, they are between high-level (labels or values significant in making decisions) and low-level ones; they are more robust because low-level features are directly related to pixel values and not robust to variations. Mid-level features are constructed from low-level ones such as SPLE [23] and Canonical correlation analysis [24]. Despite the mid-level methods to obtain values, attributed-based methods attempted to acquire description features such as narrow eyes and oval faces [25, 26].

Another track on kinship verification has been explored through metric learning algorithms, computing the similarity of kin-related faces greater than non-kin faces. One of the first activities in this approach was [27] to learn an ensemble of kernels for each class. NRML [6] attempted to make closer positive samples(kin faces) and repel negative samples(non-kin faces). It iteratively computed this action and weighed the different importance of various negative samples. Ensemble similarity learning [28] put forward a sparse similarity function to consider attributes in kin samples. Some efforts [29] learned multiple metrics from different views of features.

As deep learning has gained superiority in finding higher-level features and accuracy, the most recent research has been conducted on this approach. In [30], paired face images were patchified, patches were fed into an auto-encoder to obtain features, then the related features were mapped to a space and ultimately to a classifier. Auto-encoder [31] was also used to obtain class-specific representative features.

The paper [32] patchified face images from their landmarks to 10 patches. These patches were fed into a basic CNN, and the outputs of basic CNNs were sent to a classifier. Basic CNN consisted of three convolutional layers. VGG and triplet loss were applied by [33]. They also introduced a large kinship dataset consisting of 1000 families. They acquired features from fine-tuned VGG, reduced their dimensions with PCA, and reached 71.2 accuracy on average in the Families In the Wild (FIW) dataset. The

adaptation approach (transfer learning) from a face dataset to a kinship dataset is put forward in [34]. Its CNN consisted of five convolution layers and one fully connected (FC) layer. It fine-tuned paired face images on their first CNN network, coarse CNN with 1500 neurons in the last FC layer, and then they built two CNN networks from this coarse CNN network. These two CNN networks were again trained on Kin pairs. Their difference was that all layers of one were completely trained, and in another one, only the FC layer was trained. Eventually, NRML was applied to the features of these two networks.

Concerning the recent methods, an architecture based on the attention mechanism was designed in [35] to extract local information from face components. OR²Net [36] employed hard negative samples beyond the pre-defined protocol of configurations to utilize information of all negative samples by reweighing them. FaCoRNet [37] utilized the contrastive loss and cross-attention mechanism to pull closer facial components of kin images and pull away components of non-kin images. The research [38] introduced the usage of the curvelet transform (CLT) followed by CNN for kinship verification of children images.

Some research has been pursued in combining various aforementioned approaches called Hybrid Modeling [1]. This can be an ensemble of the same models or a combination of diverse models. Ensemble similarity learning (ESL) [28] learned a similarity function and then used it in different learners. Finally, the results of these learners were merged. JLNnet [39] utilized an ensemble of KVs for kinship identification.

In conclusion, we observe that the cutting-edge algorithms [1, 2, 8, 9] have recently been trained by parent and child face images jointly from scratch. These networks have learned a joint representation of parent-child images. Their comparison tables specify that early methods based on face representation were less accurate than their proposed method. We propose a method that elevates the accuracy of solutions based on face representation while applying graph neural network concepts.

3 Proposed Method

Human beings seek facial features and cues to find the similarity between family members [11–13]. Based on those findings of relatedness of facial components in family members and utilizing embedding vectors of face recognition systems, a method is introduced to verify their kinship, generally depicted in Fig. 1, and explained as follows:

First, CNN networks are trained on face images to acquire the embeddings. **Second**, facial image landmarks are detected, and then the face components are extracted. The embeddings of those patches are obtained through trained convolutional neural networks. **Third**, various graphs are constituted by corresponding patches between the parent and child’s face components. For example, a graph of two nodes and a bidirectional edge between a parent’s right eye and a child’s right eye is constructed. Because this graph is constructed by two corresponding components in the parent and child images, it is called a **paired graph**. There are paired graphs, of which five consist of the whole face images, right eyes, left eyes, noses, and mouths from obtaining embeddings of parent and child’s face images. Four graphs are built based on patches that do not have a face component. For example, if the right eye of the face image is

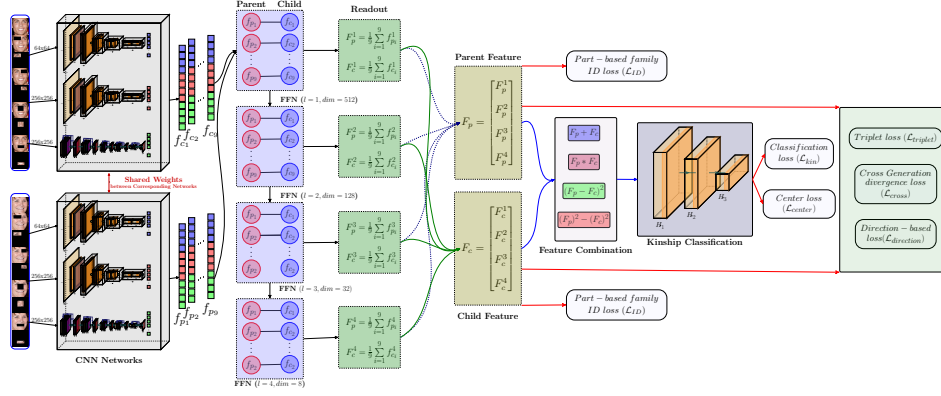


Fig. 1: The General Diagram of the Proposed Method

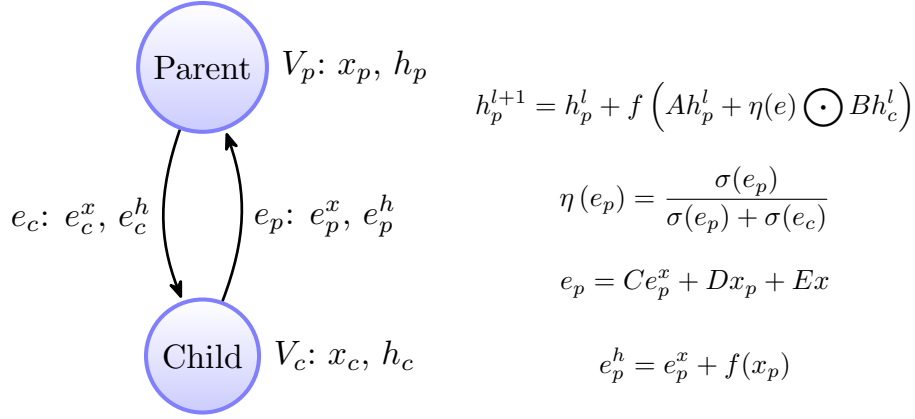


Fig. 2: A concise representation of Residual Gated Graph ConvNets for two nodes

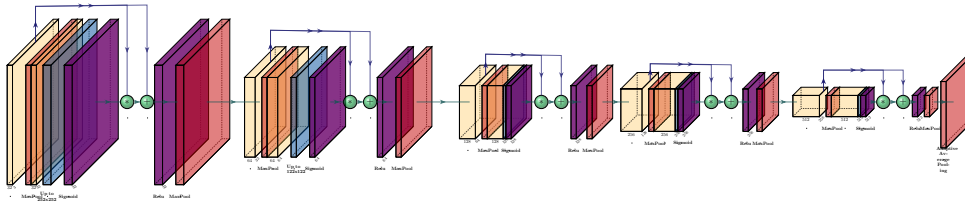


Fig. 3: The block diagram of the Extended Residual Network

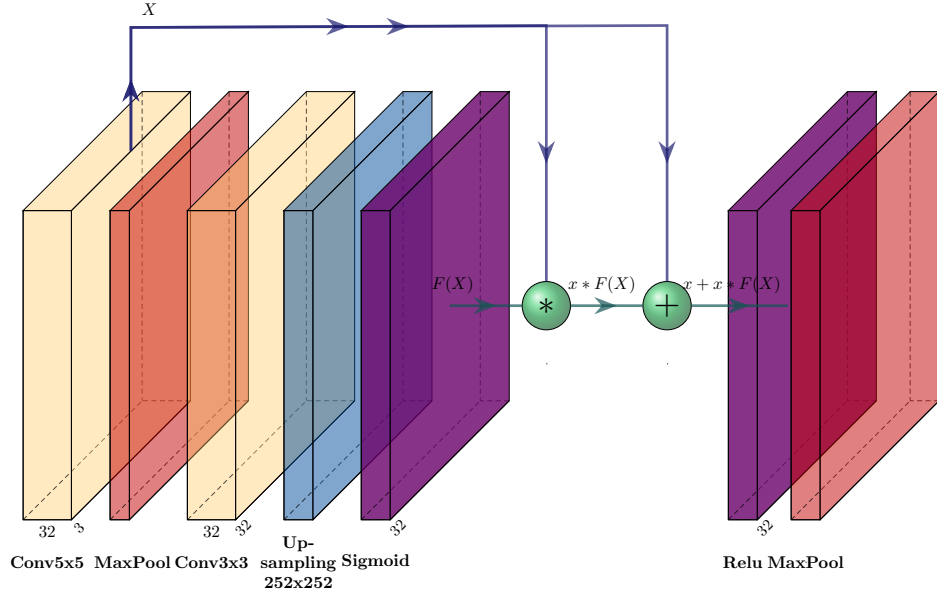


Fig. 4: One block of the Extended Residual Network (ERN)

blocked, we will have a face image without the right eye. This approach can construct four images. Then, between these four images of a parent and a child, four graphs are built. Eventually, these paired graphs constitute a forest.

Finally, This forest is fed into a kind of graph neural network called Forest Neural Network, possessing operations like GNN operations to exchange information between nodes.

The steps of the proposed algorithm are enumerated to clarify its understanding and depicted in Fig. 5.

1. Training CNN networks to obtain Embeddings
2. Landmark Detection
3. Embedding Extraction of Patches
4. Construction of Paired Graphs, i.e, a Forest
5. Training Paired Graphs by Forest Neural Network

3.1 Training CNN networks

Despite transformers having shown promising results, CNN networks still have comparative results to transformers, can generalize more, and are well-suited to limited data due to the small size of their network [40, 41]. Additionally, various CNN neural networks can be seen as expert systems and employed to enhance our knowledge about data and obtain different embedding vectors. Although various networks of the same task generally attempt to learn the equivalent data distributions, they have slightly

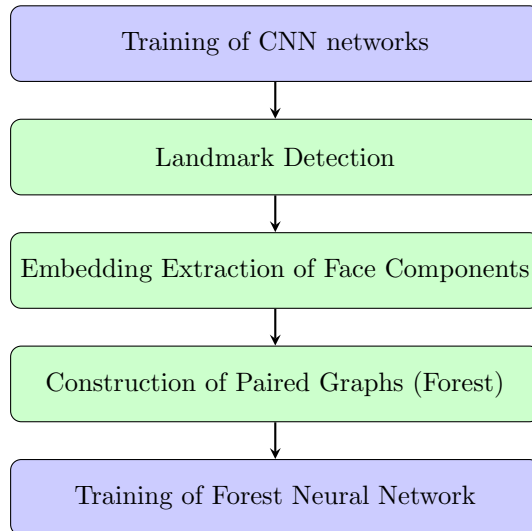


Fig. 5: The steps of the proposed algorithm

different representations since they have different performances. This slight difference is fruitful in a small sample size. Hence, we utilize various CNN networks, such as ResNet-18, which are used in different computer vision tasks, and the Extended Residual Network.

A big concern when applying CNN networks is that one sample size per identity exists in the KinFaceW-I and II. Since these datasets have a scarcity of samples, augmenting their data is required to train our network. Therefore, to train networks, we apply various augmentation techniques and masked images, such as complete face images without the right eye, left eye, nose, and mouth.

In addition, to obtain much information about faces, their high-resolution images can assist and train networks with the same neural structure. Therefore, each network can produce different representations because of various resolutions. Since face images with higher resolutions are not provided, one solution is to apply GANs to produce high-resolution images. Moreover, employing GANs has another advantage because they produce images in the same domain and remove differences between parent and child images taken under different conditions.

About choosing GANs, perceptual metrics like FID [42] and NIQE [43] can help to find a good candidate. Among the cutting-edge GANs for super-resolution, we check them based on FID and NIQE and visually their outputs and select GFP-GAN [44], a blind face restoration to produce 256x256 images. After that, the ResNet is retrained for this new dataset to gain new embeddings.

3.1.1 Extended Residual Network (ERN)

The attention mechanism among layers in [9, 35] is applied to highlight the local parts playing a significant role in kinship verification. An ERN block consists of a convolution (kernel=5x5), max-pooling, another convolution (kernel=3x3), up-sampling, and sigmoid layers applied to the combination of paired parent-child’s images as shown in Fig. 4

These consecutive operations produce a feature map with values in the range of [0-1]. This feature map is multiplied by the original to highlight the significant parts. Finally, the original feature map is added to neutralize the disappearance of some features, like the residual parts in all residual networks. The paper [9] used this attention module called the residual block for extracting shared features. However, The parent and child’s face images are separately fed to the module. Then different combinations of feature maps were used for the classification.

Despite the module usage in [9, 35], we employ this attention mechanism in finding good representations for the entire images in the dataset. Some changes must be executed to produce the embedding vector consistent with other CNN networks. If we use three layers of the attention block such as [9], a high dimensional feature map is produced and makes the whole model very large. One way to reduce the feature map’s dimension is to use the pooling layer at the end of all the attention blocks, such as an adaptive average pooling. This adaptive pooling layer at the end of the blocks results in an embedding vector of size 128, which is inconsistent with other embedding vectors. Therefore, these blocks are changed to gain an embedding vector of the size 512.

For attention block usage, our solution is to change the size of the input image to 256 by 256 since consecutive convolution operations on an image make the two last dimensions of the feature map very small. The specifications of the convolutional and up-sampling layers in all blocks are shown in Table 1 and Table 2. For abbreviation, the padding and stride of all convolution layers are not mentioned and are set to zero and one for all of them, respectively.

Table 1: Convolutional layers of all blocks. The padding and stride for all convolutional layers are 0 and 1, respectively.

Convolution Layer	In channel	Out channel	Kernel Size
the 1 st conv of block 1	3	32	(5,5)
the 2 nd conv of block 1	32	32	(3,3)
the 1 st conv of block 2	32	64	(5,5)
the 2 nd conv of block 2	64	64	(3,3)
the 1 st conv of block 3	64	128	(5,5)
the 2 nd conv of block 3	128	128	(3,3)
the 1 st conv of block 4	128	256	(5,5)
the 2 nd conv of block 4	256	256	(3,3)
the 1 st conv of block 5	256	512	(5,5)
the 2 nd conv of block 5	512	512	(3,3)

The schematic of the Extended Residual Network (ERN) is demonstrated in 3.

Table 2: Up-sampling size of all blocks

Up-sampling layer	Size
Block 1	(252,252)
Block 2	(122,122)
Block 3	(57,57)
Block 4	(24,24)
Block 5	(8,8)

3.2 Landmark Detection

To localize face components, finding landmark positions on the face image is necessary. Some famous landmark detections include MTCNN [45], and DLIB [46]. However, one of the state-of-the-art algorithms in this area is SPIGA [47] obtaining the highest result in different face detection benchmarks. Based on our experiment, all landmarks can be identified using SPIGA, whereas, for some rare images, their landmarks can not be detected by others.

If landmark detection identifies five landmarks, a bounding box for each landmark must be determined. If it produces 68 or 98 landmarks, then the bounding box of each landmark can be specified by its landmark points. The minimum and maximum points in the x and y axes define the bounding box. For example, the right eyebrow and right eye landmarks represent the right eye box.

3.3 Embedding Extraction of Patches

Four bounding boxes of the right and left eye, nose, and mouth are extracted by the coordinates found in Section Landmark Detection 3.2. In addition, the whole face image without the right eye bounding box is extracted. This image is mentioned hereafter as the face image without the right eye. In this approach, face images without a left eye, a nose, and a mouth are produced. In total, nine images are obtained for each face image. Then, the trained CNN networks are applied to acquire embedding vectors of all nine images.

3.4 Forest Graph Construction and Training

Based on the hypothesis mentioned at the beginning of Section 3, paired graphs between parent and child images are being constructed. These paired graphs construct a forest of graphs.

For training the forest graph, the CGN algorithm is operated on each paired graph separately. Then, at the end of the epoch, a mean aggregation is calculated among all parent nodes from all nine graphs. The obtained feature is considered the parent’s feature vector. By this approach, a feature vector for the child is also procured.

3.5 Details of Training Forest Graph Network

Owing to the diversity of information on face components and the hypothesis that human beings investigate people’s similarity through face components, a Forest Neural

Network (FNN) is recommended. It has operators and computations like graph neural networks, except that it contains separate graphs. This paper uses a kind of GCN known as Residual Gated Graph Convnets [48] shown in Fig. 2. Since every graph in our FNN contains only two nodes of parent and child nodes, computations of every graph in FNN are simplified as follows:

Every node has its feature vector: Some operations are performed on the initial feature vector, X , after updating, called the hidden feature vector, \mathbf{h} or the hidden representation. The hidden representations of parent and child nodes are h_p and h_c , respectively.

Every Edge of the Residual Gated Graph ConvNet also contains a feature vector, e^x , as the initial edge vector and, after updating, called e^h .

The hidden representations, h_p and h_c , for parent and child nodes are calculated by Eq. 1. All equations are written for the parent nodes, and the child nodes are alike.

$$h_p^{l+1} = h_p^l + f \left(Ah_p^l + \eta(e) \odot Bh_c^l \right) \quad (1)$$

In Eq. 1, $h_p^0 = x_p$, $h_c^0 = x_c$, and f is an activation function like ReLU. $\eta(e_p)$ is the gate term weighing the amount of information exchanged among the parent node and its neighbor, the child node, and calculated in Eq. 2

$$\eta(e_p) = \frac{\sigma(e_p)}{\sigma(e_p) + \sigma(e_c)} \quad (2)$$

To calculate the edge representation e_p , the following equation is applied:

$$e_p = Ce_p^x + Dx_p + Ex \quad (3)$$

This Eq. 3 uses the parent node information, i.e., x_p , neighboring information, x , and its incoming edge information, e^x .

$$e_p^h = e_p^x + f(x_p) \quad (4)$$

The Eq. 4 portrays that the next edge representation, e_p^h , is obtained by the previous edge representation, e_p^x , and the output of the nonlinear function on that node representation. All updates based on Eq. 1 to 4 on the nine graphs are performed.

Readout phase: the final state of FNN is the aggregation function, i.e., mean, operated to all parent nodes of the nine graphs. In other words, the mean of all parent nodes in the forest represents a feature vector for the parent in that layer, F_p^l as written in Eq. 5.

$$F_p^l = \frac{1}{9} \sum_1^9 f_{p_i}^l \quad (5)$$

Then, all these mean vectors of parent nodes from all layers are concatenated together as the final feature vector for the parent, F^p , depicted in Eq. 6.

$$F^p = \begin{bmatrix} F_p^1 \\ F_p^2 \\ F_p^3 \\ F_p^4 \end{bmatrix} \quad (6)$$

The child’s final feature vector, F^c , is also obtained alike. The final parent and child feature vectors are sent to the next block for the classification phase.

3.6 Kinship Classifier

Feature Combination: different combinations of two feature vectors can be helpful because each form of combination resembles a different metric. In addition, if we scrutinize various distance functions, we can observe that there is a form of addition, difference, and power at the core of all of them. Hence, before feeding features of the i^{th} parent-child pair extracted from 3.5 to a classifier, different combinations of features formulated in Eq. 7 are computed and concatenated together like [9].

$$F_i^{p,c} = \begin{pmatrix} (F_i^p - F_i^c)^2 \\ (F_i^p + F_i^c) \\ (F_i^p * F_i^c) \\ ((F_i^p)^2 - (F_i^c)^2) \end{pmatrix} \quad (7)$$

Classifier: We need three linear layers because the first layer accepts the diverse combinations of features and maps them to a lower dimension. Another layer, i.e., the last layer of the classifier, is needed from mapping dimension to one or two neurons to infer whether these features have any family relationship. The middle layer is required due to the center loss. Therefore, we decrease input dimensions three times: first, the dimension of features’ combinations; second, the dimension required by the center loss; and finally, the dimension of classification.

3.7 Loss Functions

Various loss functions are employed to lower the network error from different perspectives, such as [9]. Additionally, we have added the center loss to other losses owing to its effectiveness in raising the accuracy of the network. Generally, we have four various loss functions:

- Kinship pair classification and part-based family-ID losses
- Distance-based losses: Triplet and cross-generation divergence loss

- Direction-based loss
- Center loss

Their combination is formulated in Eq. 8.

$$\mathcal{L} = \mathcal{L}_{kin} + \mathcal{L}_{ID} + \mathcal{L}_{distance} + \mathcal{L}_{direction} + \mathcal{L}_{center} \quad (8)$$

The parent and child feature vectors in the i^{th} image pair are represented by F_i^p and F_i^c , respectively. The $F_i^{p,c}$ indicates the parent and child’s combined features. Additionally, y_i denotes the class label and $y_i = 1$ if the parent and child in the i^{th} image pair have kinship relation, otherwise $y_i = 0$

3.7.1 Kinship Pair Classification Loss (\mathcal{L}_{kin})

Owing to having only one neuron in the last layer of the classifier, the binary cross-entropy loss function can be utilized to calculate the amount of the network’s classification error. For the sake of numerical stability, it is better to use BCEWithLogitsLoss combining a sigmoid layer and the Binary Cross Entropy as formulated in Eq. 9. Actual and predicted labels are represented by y_i and \hat{y}_i , respectively.

$$\mathcal{L}_{kin} = -\frac{1}{N} \sum_{i=1}^N [y_i \log \sigma(\hat{y}_i) + (1 - y_i) \log(1 - \sigma(\hat{y}_i))] \quad (9)$$

3.7.2 Part-based Family-ID Loss (\mathcal{L}_{ID})

Family members have the same identity as the family. Therefore, we can assign a specific label to all family members. Hence, we assign the same label to images possessing the kinship relation, for example, the label z_i to the two images in the i^{th} image pair for the child and parent images. On the other side, It is shown in [9, 49] that if a feature vector is divided into some parts with the same identity, it improves the robustness of the network. However, the number of the optimized division must be explored. This loss is defined in Eq. 10.

$$\mathcal{L}_{ID}(F_i, z_i) = -\frac{1}{N} \frac{1}{M} \sum_{i=1}^N \sum_{j=1}^M z_i \log p(z_i | F_{i,j}) \quad (10)$$

Where the number of facial images and their parts are N and M, respectively, the F_i and $F_{i,j}$ are the feature vector, and its j-part of i^{th} image (can be the parent or child), respectively.

3.7.3 Distance-based Loss ($\mathcal{L}_{distance}$)

This distance loss contains both cross-generation and triplet losses. The *triplet loss* attempts to lower the distance between the positive and anchor samples and increase it between the negative and anchor samples. The positive and negative samples are those who have or do not have a kin relationship with the anchor. In other words,

positive samples are those that have the same family labels, and negative samples possess different labels.

$$\mathcal{L}_{triplet} = \frac{1}{N} \sum_{i=1}^N \max \left\{ \|F_i - F_{i+}\|_2^2 - \|F_i - F_{i-}\|_2^2 + \rho, 0 \right\} \quad (11)$$

Where F_i as an anchor sample represents the feature vector of the i^{th} image, the positive samples F_{i+} are those feature vectors possessing the same label as the anchor sample. The negative samples F_{i-} are like positive samples, except they have different labels. ρ is the margin, and its default value is zero. In fact, for the first part, the distance among samples with the same family-id of F_i is calculated, and for the second part, the distance among samples with the different family-id of F_i is calculated.

Cross generation divergence decreasing Loss (\mathcal{L}_{cross}): Reducing the distance among samples, i.e., parent and child feature vectors can be beneficial since these feature vectors can be classified easily in the next stage. This loss \mathcal{L}_{cross} in Eq. 12 reduces a gap between the parent and child features.

$$\mathcal{L}_{cross} = \omega_1 \mathcal{L}_{pos} + \omega_2 \mathcal{L}_{neg} \quad (12)$$

$$\mathcal{L}_{pos} = \frac{1}{n} \sum_{i=1}^n y_i * \|F_i^p - F_i^c\|_2^2 \quad (13)$$

$$\mathcal{L}_{neg} = \frac{1}{n} \sum_{i=1}^n (1 - y_i) * \|F_i^p - F_i^c\|_2^2 \quad (14)$$

Where weights, ω_1 and ω_2 denote the importance of reducing the gap among positive or negative samples.

3.7.4 Direction-based Loss ($\mathcal{L}_{direction}$)

It is worthwhile to employ the angular distance among samples to check whether they are in the same direction. One of the ways to measure the angle among features is the cosine distance defined in Eq. 15, which takes two features of the parent (F_i^p) and child (F_i^c) in the i^{th} image pair:

$$\text{Cos}(F_i^p, F_i^c) = \frac{F_i^p \cdot F_i^c}{\|F_i^p\|_2 \|F_i^c\|_2} \quad (15)$$

It will be one if they have a zero angle in the same direction. If they are in the opposite direction, angle=180°, its distance is -1. If their angle is between zero and 180°, their distance is between -1 and +1.

This direction-based loss Eq. 16 measures the angular distance between positive and negative samples so that positive samples possess the highest similarity and negative ones possess the least similarity. Hence, similar pairs must have the label $y_i = +1$,

and dissimilar ones must have the label $y_i = -1$.

$$\mathcal{L}_{direction}(\cos(F_i^p, F_i^c), y_i) = \frac{1}{n} \sum_{i=1}^n (\cos(F_i^p, F_i^c) - y_i)^2 \quad (16)$$

3.7.5 Center Loss (\mathcal{L}_{center})

This loss aims to contract the samples in the same class in the feature space and enhance the discriminatory power of the network. It learns centers in the feature map space for each class and penalizes samples that are further to these centers [50]. Except for the binary cross-entropy loss, other losses attempt to decrease the error of the innermost layers of the network, especially layers of the forest neural network. By using this loss, we can control the kinship classification module more and impose more pressure on layers of the kinship module to produce condensed features. Its formulation is represented in Eq. 17.

$$\mathcal{L}_{center} = \frac{1}{2} \sum_{i=1}^N \|H_i - C_{y_i}\|_2^2 \quad (17)$$

Where $H_i \in \mathbb{R}^d$ denotes the hidden layer output in the kinship classification module, centers $C_{y_i} \in \mathbb{R}^d$ possess the same dimension as H_i and are set initially random. Their number equals the class number; here are two classes. These centers are learned during the training phase.

3.8 Fusion of Losses

Each loss plays its role in directing the network, owing to its various perspectives?the cross entropy loss attempts to reduce the misclassification error. Moreover, the center loss attempts to guide the feature map to produce features near class centers. The direction-based loss considers the angle between features. In addition, losses such as triplet and cross-generation loss minimize the family identity of images. The scale of these losses is significant because big values can dominate smaller ones. Therefore, various combinations of these losses can impact the network’s performance.

Additionally, a loss may not contribute to the performance except during training. In the proposed network, the center loss holds this characteristic and is gradually involved in the training phase. After that, the feature map is slightly learned from some parts of the data. Thus, we introduce the temperature rate to handle this involvement as formulated in Eq. 18.

$$\mathcal{L}_{fusion} = \omega_0(\alpha^t) \cdot \mathcal{L}_{center} + \sum_{i=1}^M \omega_i \mathcal{L}_i \quad (18)$$

The temperature rate α^t at the early stage of training is small and increases in every epoch t . Every ω_i is a constant number determined by its corresponding loss. The temperature base α is also a constant number. The pseudo-code of the proposed algorithm to investigate how FNN and losses can be applied is represented in Alg. 1.

Algorithm 1 The Proposed FNN For Kinship Verification:

Require:

- ▷ x_1 and x_2 are parent and child images
- ▷ F_p, F_c are Parent and child Features from FNN.
- ▷ H is the feature of MLP for the center loss.
- ▷ n_part determines the number of division for features

Ensure:

- ▷ $epoch_loss$ shows the loss in every epoch
- ▷ $epoch_trn_acc$ denotes the current accuracy in epoch

```
1: n_data ← 0
2: epoch_loss ← 0
3: epoch_train_acc ← 0
4: for all (x1, x2, labels, parent_ids, child_ids)
5:     ∈ dataloader do
6:     Move all data to GPU
7:     ground_truth ← flatten(labels)
8:     target ← concat(parent_ids, child_ids)
9:
10:    scores, Fp, Fc, family_id, H ← FNN_Model(x1, x2)
11:    predictions ← (batch_scores > 0.5)
12:    epoch_trn_acc ← epoch_trn_acc + ...
13:    sum of all samples correctly classified
14:
15:    n_data ← n_data + n_samples_in_batch
16:    f ← concat( $F_p, F_c$ )
17:    p1, p2 ← Compute positive sample features
18:    n1, n2 ← Compute negative sample features
19:    c.similarity ← cosine_similarity( $F_p, F_c$ )
20:    Compute Losses:
21:     $\mathcal{L}_1$  ← BCE(batch_scores, ground_truth)
22:     $\mathcal{L}_2$  ← MSE(p1, p2)
23:     $\mathcal{L}_3$  ← MSE(n1, n2)
24:     $\mathcal{L}_4$  ← MSE(c.similarity, ground_truth)
25:     $\mathcal{L}_5$  ← Triplet(f, target)
26:    for  $i$  ← 1 to n_part do
27:         $\mathcal{L}_6$  ←  $\mathcal{L}_6$  + CrossEntropy(family_id, target)
28:    end for
29:     $\mathcal{L}_7$  ← CenterLoss (H, ground_truth)
30:     $\mathcal{L}_{fusion}$  ←  $\omega_0 \cdot (\alpha^t) \cdot \mathcal{L}_{center}$ 
31:    for  $i$  ← 1 to 6 do
32:         $\mathcal{L}_{fusion}$  ←  $\mathcal{L}_{fusion}$  +  $\omega_i \cdot \mathcal{L}_i$ 
33:    end for
34:    set gradients of parameters in optimizers to zero.
35:     $\mathcal{L}_{fusion}.backward()$ 
36:    optimizer.step()
37:    for all param ∈ Center_loss.parameters() do
38:        param.grad.data ← param.grad.data ·  $(\omega_0 \alpha^t)^{-1}$ 
39:    end for
40:    Center_optimizer.step()
41:    epoch_loss ← epoch_loss +  $\mathcal{L}_{fusion}$ 
42: end for
43: epoch_loss ← epoch_loss / (iter + 1)
44: epoch_trn_acc ← epoch_train_acc / n_data
45: return epoch_loss, epoch_trn_acc
```

Table 3: Various augmentation techniques with their parameters used to train CNN Networks are listed.

Augmentation Technique	Parameters	Augmentation Technique	Parameters
Flip (Horizontal)	default	Sepia	default
Random Rotate 90	default	ISO Noise	intensity=(0.1, 0.5), color_shift=(0.01,0.05)
Equalize	mode='cv', by_channels=True	Gaussian Noise	var_limit=(10.0, 50.0)
Down Scale	scale_min=0.25, scale_max=0.25, interpolation=0	Multiplicative Noise	multiplier=(0.9, 1.1), per_channel=True, elementwise=True
Hue Saturation	hue_shift_limit=(-20, 20), sat_shift_limit=(-30, 30), val_shift_limit=(-20, 20)	Random Brightness Contrast	brightness_limit=(-0.2, 0.2), contrast_limit=(-0.2, 0.2), brightness_by_max=True
Random Rain	slant_lower=-10, slant_upper=5, drop_length=10, drop_width=1, drop_color=(0, 0, 0), blur_value=2, brightness_coefficient=0.7,	Shift Scale Rotate	rotate_limit=(-45, 45), shift_limit=(-0.0625, 0.0625), scale_limit=(-0.1, 0.1), interpolation=cv2.INTER_NEAREST, border_mode=cv2.BORDER_CONSTANT, rotate_method='largest_box'

4 Experiment

This section mentions datasets and experimental configurations. First, public datasets of kinship verification are introduced, and then the implementation details and experiments for CNN networks and FNN are elucidated.

4.1 Dataset

We investigate the effectiveness of the proposed method on KinFaceW-I and KinFaceW-II [6]. These datasets provide parents and their children’s unconstrained facial images. They comprise four types of kinship relationships: Father-Son (FS) and Father-Daughter (FD), Mother-Son (MS), and Mother-Daughter (MD). KinFaceW-I owns 156, 134, 116, and 127 image pairs for each kinship type. KinFaceW-II encompasses 250 image pairs for each kinship relationship.

4.2 Configuration of CNN Networks

The implementation details for extracting embedding features from ResNet-18 and ERN are described here. Since only one sample per identity is available in KinFaceW-I and II, augmenting the number of samples through augmentation techniques is necessary. The reason for augmentation is that at least one sample for the training phase and another for the test phase is required. The Albumentation package [51] increases the number of samples. The various augmented techniques employed and their parameters in training and testing CNN networks are listed in Table 3, and produced pictures are shown in Fig 6.

It is presented in [35] that covering one of the main components of face images can improve the performance of the kinship network. Hence, we use masked face images for augmentation, such as faces without left-eye, right-eye, nose, and mouth, as shown in 7.

Eventually, all 12 augmented images, four masked ones, and the original one are used for training CNN networks. All images of every identity are randomly split into 14 and 3 for training and testing, respectively. The Adam optimizer with a learning rate of 0.00001 is used. The batch size and the epoch number are set to 16 and 200, respectively.



Fig. 6: The original child image and the other augmented pictures are in the rows from left to right and top to down in sequence: Original, Flip, Equalize, Dawn Scale, Hue Saturation, Random Rain, Sepia, ISO Noise, Gaussian Noise, Multiplicative Noise, Random Brightness Contrast, and Shift Scale Rotate.

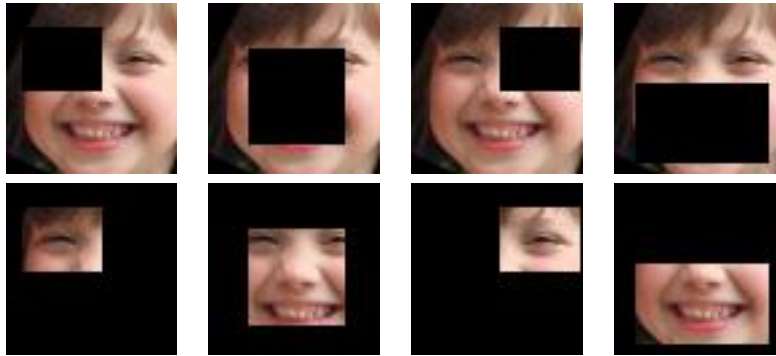


Fig. 7: The masked face images are in the rows from left to right and top to down in sequence.

The same procedure described in this section is used to train CNN networks for high-resolution images obtained by GFP-GAN [44].

4.3 Configuration of Forest Neural Network(FNN)

We follow the predefined configuration explained in [6] to have a fair comparison with other papers. Thus, every experiment for every relationship is conducted in the five-fold cross-validation with specified kin or Non-kin relations. Every fold consists of equal Kin (positive) or Non-Kin(Negative) samples. In every iteration, one fold is a test set, and the other folds are a train set. Moreover, at the beginning of every iteration, the model is preset to the initial values not to affect other iterations' results. The model's

Table 4: Comparison of the cutting-edge algorithms’ accuracy with our proposed algorithm for KinFaceW-I and II

Dataset	KinFaceW-I					KinfaceW-II				
	F-S	F-D	M-S	M-D	Mean	F-S	F-D	M-S	M-D	Mean
Method										
KML [52]	83.8	81	81.2	85	82.8	87.4	83.6	86.2	85.6	85.7
FSP [53]	74.6	74.9	78.3	86	76.8	92.3	84.5	80.3	94.8	90.2
DDMML [54]	86.4	79.1	81.4	87	83.5	87.4	83.8	83.2	83	84.3
AdvKin [55]	75.7	78.3	77.6	83.1	78.7	88.4	85.8	88	89.8	88
H-RGN [8]	81.7	78.8	81.4	88.6	82.6	90.6	86.8	93	96	91.6
DSMM [56]	81.7	76.7	82.3	89	82.4	92.6	89.8	95.8	93.6	93
D4ML [9]	87.5	79.2	80.2	88.6	83.9	91.2	87.8	93.2	96.6	92.2
FNN	82.69	79.11	77.6	88.95	82.09	94.2	91.6	92.8	96.6	93.8

Table 5: Accuracy Results of various CNN Networks and their Combinations for the KinFaceW-I dataset. The number inside the parentheses denotes the one dimension of the image size; for example, 64 denotes that the input image size is 64x64.

Embedding Network(Input Image Size)	F-S	F-D	M-S	M-D	Accuracy
ResNet(64)	73.04	66.49	66.39	75.7	70.41
ResNet(1024)	78.16	67.19	69.14	77.7	73.12
ResNet(64)+ResNet(1024)	77.91	71.31	70.63	83.77	75.91
ERN(64)	70.82	66.06	65.92	74.84	69.41
ERN(256)	71.48	64.95	70.25	79.52	71.55
ResNet(64)+ResNet(1024)+ERN(64)+ERN(256)	83.68	73.16	73.69	87.8	79.59
ResNet(64)+ResNet(1024)+ERN(256)	81.38	76.13	77.13	88.57	80.81
Ensemble of good configurations	82.69	79.11	77.6	88.95	82.09

performance is the average of five accuracy results on test sets for every kinship. The proposed method is implemented in Pytorch 2.3.0 with cuda 12.1, cudnn 8.0, and DGL 2.0.0.cu121. The learning rate, batch size, the number of epochs, and learning decay are 0.00001, 64, 70, and 0.5, respectively. The experiments are conducted on a system with an Intel(R) Core(TM) i7-2600k CPU @ 3.40GHz, 12 GB memory, NVIDIA GeForce GTX TITAN X, and Anaconda 24.5.0.

4.4 Comparison with State-of-the-Art Methods

The experimental results of our proposed method are mentioned in Table 4 for the KinfaceW-I and II datasets. Our method obtains the highest results in the KinFaceW-II and the highest for the mother-daughter relationship for the KinFaceW-I.

4.5 Discussion and Analysis

4.5.1 Effect of using various CNN Networks

To investigate the significance of each CNN Network, we conduct experiments to display the accuracy result of each network and their concatenations as embedding vectors separately as demonstrated in Tables 5 and 7 for the KinFaceW-I and II datasets, respectively.

Table 6: Good Configurations for KinFaceW-I

α	H_1	H_2	accuracy
1.04	256	8	80.93
1.05	256	8	80.81
1.07	256	8	80.58
1.06	256	8	80.44
1.03	256	8	80.32

Table 7: Accuracy Results of various CNN Networks and their Combinations for the KinFaceW-II dataset. The number inside the parentheses denotes the one dimension of the image size; for example, 64 denotes that the input image size is 64x64.

Embedding Network(Input Image Size)	F-S	F-D	M-S	M-D	Accuracy
ResNet(64)	81.6	74	78.2	82.4	79.05
ResNet(1024)	88.2	82	87.4	91	87.15
ERN(64)	81.4	76.6	78	80.6	79.15
ERN(256)	86.4	80.6	83.4	88	84.6
VGG(64)	59.6	57.8	59	56	58.1
ResNet(64)+ERN(64)	89	84.2	86.4	92.8	88.1
ResNet(1024)+ERN(256)	90.8	88.2	91.2	94.2	91.1
ResNet(1024)+ERN(256)+VGG(1024)	91.8	87.6	93.8	96.2	92.35
ResNet(1024)+ERN(256)+VGG(64)	92.4	88.6	92.8	95.6	92.35
ResNet(64)+ERN(64)+VGG(64)	93.8	90	93	96	93.2
Ensemble of good configurations	94.2	91.6	92.8	96.6	93.8

Table 8: Good Configurations for KinFaceW-II

α	H_1	H_2	accuracy
1.02	256	8	93.3
1.05	256	8	93.2
1.05	256	16	93.15
1.05	128	8	93.05
1.05	256	16	92.95

The general experiment setting is changed only for dimensions to feed the embeddings to the FNN. Hyper-parameters are the same as the general optimal values (such as $\alpha = 1.05$ and $\omega_0 = 0.01$). The parameters of the ensemble for KinFaceW-I and II are mentioned in Table 6 and Table 8, respectively.

Results manifest that each CNN impacts the result, and various combinations of CNN Networks can enhance the accuracy because each CNN network operates as an expert. Mixing varying experts can improve accuracy since each attempt to classify data from different perspectives. Another explanation is that diverse CNNs represent the data distribution with variant views.

4.5.2 Effect of the Center Loss

It is essential to assess whether the center loss can affect the accuracy of the kinship verification. If its presence does not raise the accuracy, it does not need to be included in the combination of losses. Therefore, we conduct experiments to investigate its presence in the loss fusion.

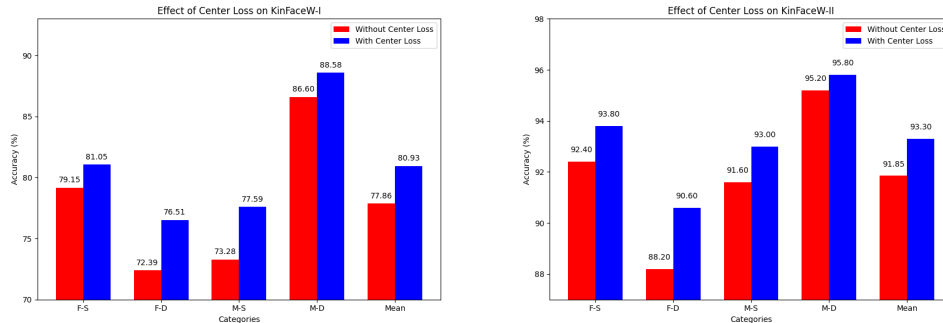


Fig. 8: Results of our proposed method with and without using the center loss on the KinFaceW-I and KinFaceW-II datasets.

The results of the KinFaceW-I and KinFaceW-II for the presence or absence of the center loss in the fusion of losses are demonstrated in Fig. 8. Its presence can improve accuracy in all kinship types. For example, it improves the accuracy of FS:1.9, FD:4.12, MS:4.31, and MD:1.98, and the improving mean of all types' accuracy is 3.07. It contributes accuracy of at least nearly 2 percent and generally 3 percent in the KinFaceW-I dataset. In addition, it enhances the accuracy of FS:1.4, FD:2.4, MS:1.4, and MD:0.6, and the improving mean of all types' accuracy is 1.45 in the KinFaceW-II dataset.

Therefore, adding the center loss can enhance the accuracy by nearly 2 percent when it is combined correctly with other losses.

4.5.3 Hyper-parameter Analysis

Hyper-parameters in our method belong to the fusion of different loss functions that need to be analyzed and found to have optimal values since they can scale losses and weigh their impacts on the model.

The weights ω_i match D4ML [9] and play the same functionality and performance in our work. We have two hyper-parameters ω_0 and α to investigate for the center loss. Our optimization approach is that all other hyper-parameters are fixed except the one we want to find. The accuracy reported is the mean of all kinship types.

- *Impact of ω_0 :*

The figure 9 denotes that the various values of the initial parameter are examined through $[0.001, 0.1]$, and the value 0.01 is the optimum since other values degrade the accuracy.

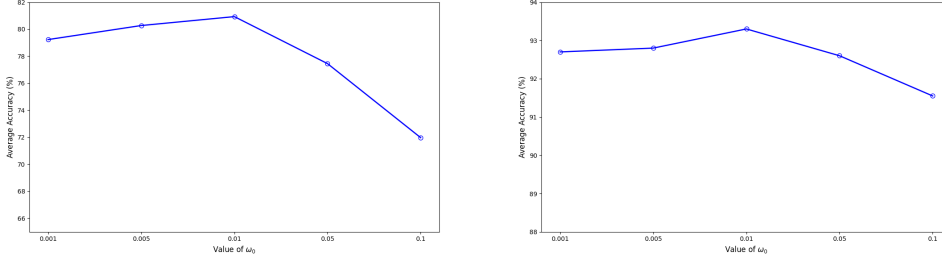


Fig. 9: The initial Temperature for KinFaceW-I and II. The different values of the initial temperature are investigated while other parameters are fixed.

- *Impact of α :*

The search range of the optimal value for the temperature rate α is $[1, 1.1]$ for KinFaceW-I and KinFaceW-II represented in Fig. 10. The optimal values for KinFaceW-I are 1.04 and 1.05, and for KinFaceW-II are 1.02 and 1.05. The value 1.05 for the temperature rate is selected since it is a frequent value of acquiring high accuracy in both datasets. Values less than one do not make sense because these values gradually disappear the impact of the center loss. Values greater than 1.10 degrade the accuracy noticeably more and are not depicted in Fig. 10.

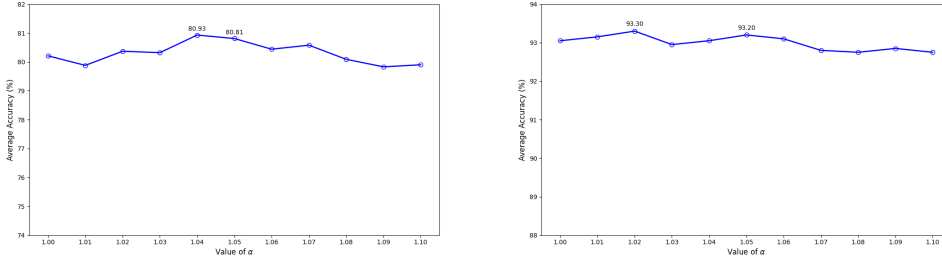


Fig. 10: The Temperature Rate α for KinFaceW-I and KinFaceW-II. The optimal values of KinFaceW-I are attained at 1.04 and 1.05 in order, and of KinFaceW-II at two points, 1.02 and 1.05 in order.

Table 9: Various sizes of the first and second hidden layers.

$H_1 \backslash H_2$	8	16	32	64
128	93.05	92.95	92.8	92.5
192	92.4	92.45	92.7	92.35
256	93.2	93.15	92.55	92.3
512	92.4	92.5	92.15	91.8

Table 10: Comparison of Model Size

Method	#Parameters	Total Size(MB)
D4ML	91,328,881	462.78
ResNet	2,767,521	10.56
ERN(128)	344,465	1.31
ERN(256)	908,641	3.47
VGGFACE	31,931,321	121
FNN(KinFace-I)	19,090,920	72.83MB
FNN(KinFace-II)	54,741,259	208.82MB

4.5.4 Architecture of Kinship Classification

In the beginning, two fully connected layers without any hidden layers are designed. However, when the center loss is incorporated in companion with the binary cross entropy loss in this network, the center loss can not help to enhance the accuracy. Hence, the kinship classification module must be re-designed to utilize the center loss and increase the accuracy. Therefore, hidden layers are added to the classification module. The main reason is that we want the center loss to impact the spread of classes in the feature space. Features from these hidden layers are fed into the center loss. Additionally, the size of the input layers is enormous, and the output layer comprises one or two neurons. Hence, the first hidden layer is assumed to be bigger than the second. Nonetheless, the sizes of these hidden layers are hyper-parameters that must be examined. The various values of the hidden layers are probed and illustrated in Table 9. When the sizes of these layers are (256,8) or (256,16), the mean accuracy of all relationships is the highest.

4.5.5 Comparison of Model Size

We compare our model size with the D4ML algorithm and present that our proposed model is much smaller and its training time is lower in Table 10. The torchinfo package obtains these parameters.

5 Conclusion and Future Work

We introduced an innovative approach that leverages face classification algorithms for kinship verification through their face representations and incorporates graph neural network operators. Our proposal denotes how to apply each CNN network as an

expert system and combine their outputs with the forest neural network. We have developed an algorithm that considers the disjoint nature of face components and fuses their outcomes to increase verification accuracy through the forest neural network and center loss. Employing these methods, we have achieved accuracy on par with the cutting-edge. This result should provide reassurance about the effectiveness of our approach.

Moreover, we provide a new combination of loss functions, especially the center loss, to gradually engage in training our architecture and indicate the structure of the kinship classification module so that the output of the fully connected layers is used in the center loss.

In addition, we reveal the effectiveness of high-resolution images for KinfaceW-I since they were gathered from various photos. Converting them to high resolution can mitigate their differences and enhance their accuracy.

For future work, we envision exploring various combinations of other popular networks, which could potentially increase the accuracy of kinship verification. Furthermore, the investigation of hyper-parameters and parameters for end-to-end learning of the proposed architecture could lead to significant advancements in the field.

6 Ethical Approval

Not applicable

7 Consent to Participate

Not applicable

8 Consent to Publish

Not applicable

9 Data Availability Statement

All datasets used in this research are famous benchmarks that are freely available on the Internet.

10 Authors Contributions

Ali Nazari proposed ideas, wrote codes, conducted experiments, and wrote the paper. Omidreza Borzoei conducted experiments and wrote some parts of codes. Mohsen Ebrahimi-Moghaddam supervised the entire research.

11 Funding

There was no fund for this research.

12 Competing Interests

The authors declare that they have no conflict of interest.

References

- [1] Mzoughi, M.C., Aoun, N.B., Naouali, S.: A review on kinship verification from facial information. *The Visual Computer*, 1–21 (2024)
- [2] Wu, X., Feng, X., Cao, X., Xu, X., Hu, D., López, M.B., Liu, L.: Facial kinship verification: A comprehensive review and outlook. *International Journal of Computer Vision* **130**(6), 1494–1525 (2022)
- [3] Robinson, J.P., Shao, M., Fu, Y.: Survey on the analysis and modeling of visual kinship: A decade in the making. *IEEE Transactions on Pattern Analysis and Machine Intelligence* **44**(8), 4432–4453 (2021)
- [4] Xia, S., Shao, M., Luo, J., Fu, Y.: Understanding kin relationships in a photo. *IEEE Transactions on Multimedia* **14**(4), 1046–1056 (2012)
- [5] Kumar, C., Ryan, R., Shao, M.: Adversary for social good: Protecting familial privacy through joint adversarial attacks. In: *Proceedings of the AAAI Conference on Artificial Intelligence*, vol. 34, pp. 11304–11311 (2020)
- [6] Lu, J., Zhou, X., Tan, Y.-P., Shang, Y., Zhou, J.: Neighborhood repulsed metric learning for kinship verification. *IEEE transactions on pattern analysis and machine intelligence* **36**(2), 331–345 (2013)
- [7] Bisogni, C., Narducci, F.: Kinship recognition: how far are we from viable solutions in smart environments? *Procedia Computer Science* **198**, 225–230 (2022)
- [8] Li, W., Lu, J., Wuerkaixi, A., Feng, J., Zhou, J.: Reasoning graph networks for kinship verification: from star-shaped to hierarchical. *IEEE Transactions on image processing* **30**, 4947–4961 (2021)
- [9] Zhu, X., Li, C., Chen, X., Zhang, X., Jing, X.-Y.: Distance and direction based deep discriminant metric learning for kinship verification. *ACM Transactions on Multimedia Computing, Communications and Applications* **19**(1s), 1–19 (2023)
- [10] Kohli, N., Vatsa, M., Singh, R., Noore, A., Majumdar, A.: Hierarchical representation learning for kinship verification. *IEEE Transactions on Image Processing* **26**(1), 289–302 (2016)
- [11] Hansen, F., DeBruine, L.M., Holzleitner, I.J., Lee, A.J., O’Shea, K.J., Faslolt, V.: Kin recognition and perceived facial similarity. *Journal of Vision* **20**(6), 18–18 (2020)

- [12] Cole, J.B., Manyama, M., Larson, J.R., Liberton, D.K., Ferrara, T.M., Riccardi, S.L., Li, M., Mio, W., Klein, O.D., Santorico, S.A., *et al.*: Human facial shape and size heritability and genetic correlations. *Genetics* **205**(2), 967–978 (2017)
- [13] Dal Martello, M.F., Maloney, L.T.: Where are kin recognition signals in the human face? *Journal of Vision* **6**(12), 2–2 (2006)
- [14] Liang, J., Hu, Q., Dang, C., Zuo, W.: Weighted graph embedding-based metric learning for kinship verification. *IEEE Transactions on Image Processing* **28**(3), 1149–1162 (2018)
- [15] Fang, R., Tang, K.D., Snavely, N., Chen, T.: Towards computational models of kinship verification. In: 2010 IEEE International Conference on Image Processing, pp. 1577–1580 (2010). IEEE
- [16] Bottinok, A., Islam, I.U., Vieira, T.F.: A multi-perspective holistic approach to kinship verification in the wild. In: 2015 11th IEEE International Conference and Workshops on Automatic Face and Gesture Recognition (FG), vol. 2, pp. 1–6 (2015). IEEE
- [17] Zhou, X., Lu, J., Hu, J., Shang, Y.: Gabor-based gradient orientation pyramid for kinship verification under uncontrolled environments. In: Proceedings of the 20th ACM International Conference on Multimedia, pp. 725–728 (2012)
- [18] Guo, G., Wang, X.: Kinship measurement on salient facial features. *IEEE Transactions on Instrumentation and Measurement* **61**(8), 2322–2325 (2012)
- [19] Kohli, N., Singh, R., Vatsa, M.: Self-similarity representation of weber faces for kinship classification. In: 2012 IEEE Fifth International Conference on Biometrics: Theory, Applications and Systems (BTAS), pp. 245–250 (2012). IEEE
- [20] Puthenputhussery, A., Liu, Q., Liu, C.: Sift flow based genetic fisher vector feature for kinship verification. In: 2016 IEEE International Conference on Image Processing (ICIP), pp. 2921–2925 (2016). IEEE
- [21] Wang, X., Guo, G., Rohith, M., Kambhamettu, C.: Leveraging geometry and appearance cues for recognizing family photos. In: 2015 11th IEEE International Conference and Workshops on Automatic Face and Gesture Recognition (FG), vol. 1, pp. 1–8 (2015). IEEE
- [22] Nader, N., El-Gamal, F.E.-Z.A., Elmogy, M.: Enhanced kinship verification analysis based on color and texture handcrafted techniques. *The Visual Computer* **40**(4), 2325–2346 (2024)
- [23] Zhou, X., Hu, J., Lu, J., Shang, Y., Guan, Y.: Kinship verification from facial images under uncontrolled conditions. In: Proceedings of the 19th ACM

- International Conference on Multimedia, pp. 953–956 (2011)
- [24] Chen, X., An, L., Yang, S., Wu, W.: Kinship verification in multi-linear coherent spaces. *Multimedia Tools and Applications* **76**, 4105–4122 (2017)
- [25] Xia, S., Shao, M., Fu, Y.: Toward kinship verification using visual attributes. In: *Proceedings of the 21st International Conference on Pattern Recognition (ICPR2012)*, pp. 549–552 (2012). IEEE
- [26] Zhang, M.-L., Wu, L.: Lift: Multi-label learning with label-specific features. *IEEE transactions on pattern analysis and machine intelligence* **37**(1), 107–120 (2014)
- [27] Somanath, G., Kambhamettu, C.: Can faces verify blood-relations? In: *2012 IEEE Fifth International Conference on Biometrics: Theory, Applications and Systems (BTAS)*, pp. 105–112 (2012). IEEE
- [28] Zhou, X., Shang, Y., Yan, H., Guo, G.: Ensemble similarity learning for kinship verification from facial images in the wild. *Information Fusion* **32**, 40–48 (2016)
- [29] Hu, J., Lu, J., Tan, Y.-P.: Sharable and individual multi-view metric learning. *IEEE transactions on pattern analysis and machine intelligence* **40**(9), 2281–2288 (2017)
- [30] Dehghan, A., Ortiz, E.G., Villegas, R., Shah, M.: Who do i look like? determining parent-offspring resemblance via gated autoencoders. In: *Proceedings of the IEEE Conference on Computer Vision and Pattern Recognition*, pp. 1757–1764 (2014)
- [31] Kohli, N., Yadav, D., Vatsa, M., Singh, R., Noore, A.: Supervised mixed norm autoencoder for kinship verification in unconstrained videos. *IEEE Transactions on Image Processing* **28**(3), 1329–1341 (2018)
- [32] Zhang12, K., Huang, Y., Song, C., Wu, H., Wang, L., Intelligence, S.M.: Kinship verification with deep convolutional neural networks. In: *In British Machine Vision Conference (BMVC)* (2015)
- [33] Robinson, J.P., Shao, M., Wu, Y., Fu, Y.: Families in the wild (fiw) large-scale kinship image database and benchmarks. In: *Proceedings of the 24th ACM International Conference on Multimedia*, pp. 242–246 (2016)
- [34] Duan, Q., Zhang, L., Zuo, W.: From face recognition to kinship verification: An adaptation approach. In: *Proceedings of the IEEE International Conference on Computer Vision Workshops*, pp. 1590–1598 (2017)
- [35] Yan, H., Wang, S.: Learning part-aware attention networks for kinship verification. *Pattern Recognition Letters* **128**, 169–175 (2019)
- [36] Li, H., Zhao, X., Wang, M., Song, H., Sun, F.: Or2net: Online re-weighting relation network for kinship verification. *Expert Systems with Applications* **255**, 124815

(2024)

- [37] Su, W., Chen, M.-H., Wang, C.-Y., Lai, S.-H., Chen, T.P.-C.: Kinship representation learning with face componential relation. In: Proceedings of the IEEE/CVF International Conference on Computer Vision, pp. 3105–3114 (2023)
- [38] Oruganti, M., Meenpal, T., Majumder, S.: Kinship verification in childhood images using curvelet transformed features. *Computers and Electrical Engineering* **118**, 109375 (2024)
- [39] Wang, W., You, S., Gevers, T.: Kinship identification through joint learning using kinship verification ensembles. In: *Computer Vision—ECCV 2020: 16th European Conference, Glasgow, UK, August 23–28, 2020, Proceedings, Part XXII 16*, pp. 613–628 (2020). Springer
- [40] Maurício, J., Domingues, I., Bernardino, J.: Comparing vision transformers and convolutional neural networks for image classification: A literature review. *Applied Sciences* **13**(9), 5521 (2023)
- [41] Talib, M.S.M., Samsuri, M.H., Yuen, S.L., Lau, P.Y., Wong, C.W., Kamarudin, N.A., Hon, H.W.: Performance comparison of convolutional and transformer neural networks in defect classification for industrial images. In: *2024 21st International Conference on Electrical Engineering/Electronics, Computer, Telecommunications and Information Technology (ECTI-CON)*, pp. 1–6 (2024). IEEE
- [42] Heusel, M., Ramsauer, H., Unterthiner, T., Nessler, B., Hochreiter, S.: Gans trained by a two time-scale update rule converge to a local nash equilibrium. *Advances in neural information processing systems* **30** (2017)
- [43] Mittal, A., Soundararajan, R., Bovik, A.C.: Making a “completely blind” image quality analyzer. *IEEE Signal processing letters* **20**(3), 209–212 (2012)
- [44] Wang, X., Li, Y., Zhang, H., Shan, Y.: Towards real-world blind face restoration with generative facial prior. In: *Proceedings of the IEEE/CVF Conference on Computer Vision and Pattern Recognition*, pp. 9168–9178 (2021)
- [45] Zhang, K., Zhang, Z., Li, Z., Qiao, Y.: Joint face detection and alignment using multitask cascaded convolutional networks. *IEEE signal processing letters* **23**(10), 1499–1503 (2016)
- [46] Kazemi, V., Sullivan, J.: One millisecond face alignment with an ensemble of regression trees. In: *Proceedings of the IEEE Conference on Computer Vision and Pattern Recognition*, pp. 1867–1874 (2014)
- [47] Prados-Torreblanca, A., Buenaposada, J.M., Baumela, L.: Shape preserving facial landmarks with graph attention networks. In: *33rd British Machine Vision Conference 2022, BMVC 2022, London, UK, November 21-24, 2022*, p. . BMVA Press,

London, UK (2022). <https://bmvc2022.mpi-inf.mpg.de/0155.pdf>

- [48] Bresson, X., Laurent, T.: Residual gated graph convnets. arXiv preprint arXiv:1711.07553 (2017)
- [49] Sun, Y., Xu, Q., Li, Y., Zhang, C., Li, Y., Wang, S., Sun, J.: Perceive where to focus: Learning visibility-aware part-level features for partial person re-identification. In: Proceedings of the IEEE/CVF Conference on Computer Vision and Pattern Recognition, pp. 393–402 (2019)
- [50] Wen, Y., Zhang, K., Li, Z., Qiao, Y.: A discriminative feature learning approach for deep face recognition. In: Computer vision—ECCV 2016: 14th European Conference, Amsterdam, the Netherlands, October 11–14, 2016, Proceedings, Part VII 14, pp. 499–515 (2016). Springer
- [51] Buslaev, A., Iglovikov, V.I., Khvedchenya, E., Parinov, A., Druzhinin, M., Kalinin, A.A.: Albumentations: Fast and flexible image augmentations. *Information* **11**(2) (2020) <https://doi.org/10.3390/info11020125>
- [52] Zhou, X., Jin, K., Xu, M., Guo, G.: Learning deep compact similarity metric for kinship verification from face images. *Information Fusion* **48**, 84–94 (2019)
- [53] Dawson, M., Zisserman, A., Nellåker, C.: From same photo: Cheating on visual kinship challenges. In: Asian Conference on Computer Vision, pp. 654–668 (2018). Springer
- [54] Lu, J., Hu, J., Tan, Y.-P.: Discriminative deep metric learning for face and kinship verification. *IEEE Transactions on Image Processing* **26**(9), 4269–4282 (2017)
- [55] Zhang, L., Duan, Q., Zhang, D., Jia, W., Wang, X.: Advkin: Adversarial convolutional network for kinship verification. *IEEE transactions on cybernetics* **51**(12), 5883–5896 (2020)
- [56] Li, W., Wang, S., Lu, J., Feng, J., Zhou, J.: Meta-mining discriminative samples for kinship verification. In: Proceedings of the IEEE/CVF Conference on Computer Vision and Pattern Recognition, pp. 16135–16144 (2021)